RSC Advances

ROYAL SOCIETY OF CHEMISTRY

www.rsc.org/advances

Journal Name

ARTICLE

Bipyridine type Co-complexes as hole-transporting material dopants in Perovskite Solar Cells

Received 00th January 20xx,
Accepted 00th January 20xx

DOI: 10.1039/x0xx00000x

www.rsc.org/

Jiajiu Ye[a,b] ,Li Zhou[a] ,Liangzheng Zhu[a,b], Xuhui Zhang[a,b], Zhipeng Shao[a], Xu Pan*[a] ,Songyan Dai*[c]

Hole-transporting materials (HTM) have significant effect on solar cell properties and cobalt complex commonly used as dopant in HTM layer. The molecular structure of ligand always has an important influence on dopant capability. In this work, a series of cobalt complexes of substituted bipyridine dopant were synthesized by modification of the molecular structure and investigated as possible dopant alternatives. The electron conductive ability and redox potential was tested by characterizing their absorption spectroscopy and conductivity properties, the best dopant based on tris(4,4'-di-tert-butyl-2,2'-dipyridyl)-cobalt(III) tris[bis(trifluoromethylsulfonyl)-imide], resulted in power conversion efficiency up to 14.91% measured under standard solar conditions (AM 1.5G, 100 mW /cm2). In addition, the co-solvent of dichloroethane and acetyl acetone was specifically selected for the bipyridine type dopants due to its better solubility for both spiro and dopant. Because of easy acquisition of the ligand and the simplicity of complexes synthesis, this dopant represents practical alternative as efficient dopant for hole-transporting material in perovskite solar cells.

Introduction

In recent years Organic-inorganic hybrid solar cells as a new branch of solar cells has achieved rapid development[1-5] .In 2009, Miyasaka research team successfully prepared the first perovskite solar cell using organic-inorganic hybrid material, and achieved the power conversion efficiency of 3.8%. In 2012, Park etal reported spiro-OMeTAD as HTM used in solid state organic/inorganic perovskite solar cells (PSC) to replace liquid ones and got a photoelectric conversion efficiency of 9.7% [6].Up to now, the efficiency of PSCs have exceeded more than 20%[7-9].

In perovskite solar cell, HTM layer is important to the overall performance[10,11] and tremendous improvements about HTMs have been made in order to achieve high efficiency solar cells[12-14]. Among all the HTMs, spiro-OMeTAD (2', 7, 7'-tetrakis-(N, N-di-p-metho xyphenylamine) -9, 9'-spirobifluorene) is widely used in perovskite-based photovoltaic devices. The pristine form of spiro-OMeTAD possesses low conductivity which would lead to low charge mobility and high series resistance. In order to solve the problem, an effective method of doping was used. Studies have shown that the key factors which affecting efficient doping were the conductivity of the pure materials and its redox state; the increasing oxidized state spiro-OMeTAD$^+$ can enhance the conductivity, which will directly affect the performance of the device[15-18]. So far a series of effective cobalt dopants have been developed, all of these dopants will allow devices to exhibit excellent performance. Co(III) Complexes of tris[2-(1H-pyrazol-1-yl)-4-tert-butylpyridine) cobalt(III) tris(bis(trifluoromethylsulfonyl) imide)] (FK209) was used earlier in Solid-State Dye-Sensitized Solar Cells by Burschka[19]. In 2013, Noh made use of FK209 as dopants in spiro system and achieved PCE of 10.4%,due to the effect between the co-complex and Li-TFSI in conjunction with spiro-OMeTAD[20]. Koh developed a pyrimidine core cobalt dopant with deep redox potential named MY11 ,an overall power conversion efficiency of 12% was achieved using as p-type dopant to spiro-OMeTAD[21]. In addition, the role of the solvent is also important. Xu reported a low-cost, chlorinated, organic solvent, 1,1,2,2-tetrachloroethane (TeCA) used as a co-solvent and an effective additive for the triarylamine-based organic HTM and significantly increased the electrical conductivity, a record power conversion efficiency (PCE) of 7.7% was obtained [22].

Despite the obvious effect of dopant, it still has defects. Some of cobalts reacted with organic host and the color of HTM solution became dark that will absorb light and result in the competition with photosensitizer. Some of these dopants have poor solubility in organic solvents or possessed high boiling point, making them difficult for the photovoltaic devices fabrication. Due to the complex synthetic method and high cost, most of the dopants are not easy to obtain which would limit large-scale production. Therefore studies of low-cost, reaction-colorless, good solubility and easy acquisition dopants for HTMs are still necessary.

In this work we reported a number of cobalt complexes of substituted bipyridine with that have been synthesized from

[a] Key Laboratory of Novel Thin-Film Solar Cells, Institute of Applied Technology, Hefei Institutes of Physic Science, Chinese Academy of Sciences, Hefei 230031
[b] University of Science and Technology of China, Hefei 230026, China
[c] State Key Laboratory of Alternate Electrical Power System with Renewable Energy Sources, North China Electric Power University, Beijing 102206, China
Supplementary Information (ESI) available: [details of any supplementary information available should be included here]. See DOI: 10.1039/x0xx00000x

solution and are particularly promising due to their chemical properties of ambient stability, easy preparation, and the possibility to change organic host chemical and physical properties. These cobalt complexes were employed as possible alternatives dopant for spiro-OMeTAD in Perovskite Solar Cells. In addition, we employed dichloroethane and acetyl acetone co-solvent as HTM solvent, the dopant expressed more efficient to dope the triarylamine-based hole-conductors due to the solubility improved and synergistic reaction between co-solvent and dopant. An efficiency of 14.91% has been obtained with a J_{sc} of 19.52 mA/cm2, V_{oc} of 1.02 V, and *FF* of 74.96% based on tris(4,4'-di-tert-butyl-2,2'-dipyridyl)-cobalt(III)tris[bis(trifluoromethylsulfonyl)-imide](D1).It provides new alternatives for the fabrication low-cost and efficient perovskite solar cell.

Experimental

Synthesis of cobalt complexes

All of the complexes depicted in Fig (1) were synthesized and purification using the similar procedure. In short, 3 molar equivalents of ligand was dissolved in methanol and water mixture solvent with magnetic stirring and heated to 60 ^{o}C.The amount of methanol and water was adjusted according to the ligand solubility and the scale of the reaction so that the ligand was totally dissolved. Then 1 molar equivalent of cobalt (II) perchlorate hexahydrate was added, stirred for 30-60 minutes. After the mixture cooled to room temperature, H_2O_2 and HCl were added at 5 minutes intervals sequentially in order to oxidize the divalent cobalt and the mixture was heated at 75 ^{o}C for 2 hours. Followed by concentrated solution lithium bis (tri-fuoromethanesulfonyl) imide water solution was added slowly in the beginning at room temperature to precipitate the crude product, filtered and dried at 60 ^{o}C. The resulting compound was re-dissolved in methanol at 60 ^{o}C and then cooled down to 5 ^{o}C, the crystallized solid was just the purified product (a solid that varied from light brown to yellow).The product was characterized by H^1-NMR and element analysis (Details were described in ESI).

Solar cell device fabrication

A thick dense blocking layer of TiO_2 (bl-TiO_2) was deposited onto a F-doped SnO_2 (FTO) substrate by spin coating to prevent direct contact between the FTO and the hole-conducting layer. It was carried out using a blocking layer precursor solution prepared from titanium(IV) isopropoxide $Ti[OCH(CH_3)_2]_4$ mixed with 2-methoxyethanol ($CH_3OCH_2CH_2OH$) and ethanolamine ($H_2NCH_2CH_2OH$) according to a reported method[23] and then the film was calcined at 500 ^{o}C. A mesoporous TiO_2 layer (dysol, particle size: about 30 nm, crystalline phase: anatase) about 200 nm thickness film was deposited by spin coating at 3000 rpm for 30 s onto the bl-TiO_2/FTO substrate and calcined at 500 ^{o}C to remove organic components. The films were then immersed into 50 mM $TiCl_4$ aqueous solution diluted by cool water at 65 ^{o}C for 0.5 h and were then heated to 500 ^{o}C to repair the surface of mesoporous TiO_2 and improve the interfacial contact. The prepared MAI powders and PbI_2 (Aldrich) for 1.1M $MAPbI_3$ solution were stirred in a mixture of DMSO and DMF (8.5:1.5 v/v) at 60 ^{o}C for 1h. The resulting solution was coated onto the mp-TiO_2/bl-TiO_2/FTO substrate by a consecutive two-step spin-coating process at 1000 and 6000 r.p.m for 20 s and 30 s respectively. During the second spin-coating step at last 10s, the substrate was treated with toluene drop-casting to form the perovskite crystal.CH_3NH_3I was synthesized from hydroiodic acid reacting with methylamine according to reference[3]. The HTM layer was deposited by spin-coating at 4000 rpm for 20 s, using a solution of spiro-MeOTAD, 4-tert-butylpyridine, and lithium bis (trifluoromethylsulphonyl) imide and the Co (III)-complex in dichloroethane/acetylacetone. Finally, Gold (80 nm) counter electrode was deposited by thermal evaporation on top of the device to form the back contact.

Characterization

The conductance of spiro-OMeTAD complexes was measured by Four-Point Probes tester (RTS-9). Spiro-OMeTAD with dopants films on glass substrates, the thickness of spiro-OMeTAD films is about 250 nm deposited on glass substrate. The PCE and J–V curves were measured by using a solar simulator (Newport, Oriel Class A, 91195A) with a source meter (Keithley 2420) at 100 mA/cm^2 illumination AM 1.5G and a calibrated Si-reference cell certified by NREL. The J–V curves for all devices were measured by masking the active area with a black mask 0.09 cm^2.UV–vis absorption spectra were recorded on a UV-vis spectrometer (Hitachi U-3300). Spiro-MeOTAD and addictives were dissolved in co-solvent. Incident photon to current efficiency (IPCE) were confirmed as a function of wavelength from 300 to 800 nm (PV Measurements, Inc.), with dual Xenon/quartz halogen light source, measured in DC mode with no bias light used. The setup was calibrated with a certified silicon solar cell (Fraunhofer ISE) prior to measurements. Transient absorption spectra (TA) was record on LK80 (Applied photophysics) . The cells were measured before evaporating gold counter with a pump light wavelength of 500 nm and a probe light wavelength of 1100 nm. Repetition rate of 5Hz, the energy of laser device is 150μJ/cm^2.

Results and discussion

In the mesoscopic $MAPbI_3$ perovskite solar cell, the pores of mesoscopic TiO_2 layer are infiltrated by $MAPbI_3$ perovskite crystal. On top of the mesoscopic TiO_2, there is a thin overlayer of perovskite where HTM is covered. The electron-hole pairs are generated by $MAPbI_3$ photosensitizer, and the generated electrons and holes are transported into the mesoscopic TiO_2 and HTM layer respectively upon illumination of light. Therefore, the device will perform better if the HTM could extract the holes from the $MAPbI_3$ perovskite layer effectively. Earlier researches have already reported cobalt compounds, such as FK102, FK269, FK209, MY11 etc can be used as efficient p-dopants for HTM. The introduction of these dopants in HTM layer is well-known to increase the

conductivity in order to reduce the series resistances as well as the charge-transfer resistance at the interface between HTM layer and perovskite layer. The dopant also can be used as assist to transform the reduced state of spiro-MeOTAD to oxidation state. By incorporating different substituents, various cobalt complexes have been synthesized and used as dopants are shown in fig (1).

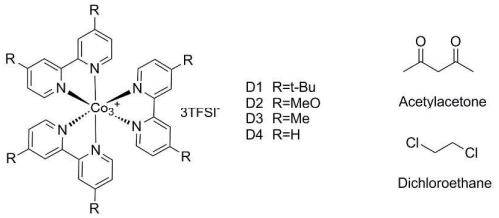

Fig.1 Structure of cobalt complex with different organic groups and composition of co-solvent

It is known that the hole conductivity of HTM layer will affect the overall device performance and we believe that the additives will increase the conductivity and lead enhancement of overall device performance .In order to understand the effect of doping, we measured the conductivity of spiro-OMeTAD films by using four-probe electrical conductivity measurements following a published procedure[15, 17, 18, 21].

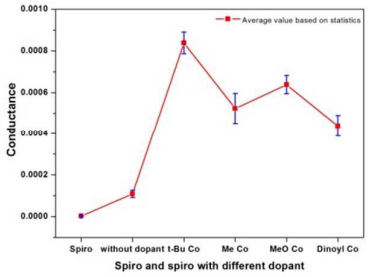

Fig.2 Average conductance value of spiro-OMeTAD with dopants films on glass substrates, the thickness of spiro-OMeTAD films is about 250 nm deposited on glass substrate. Conductance values had been normalized relative to the pristine spiro-OMeTAD film.

The results are shown in fig (2), average conductance values of spiro-OMeTAD films had been tested based on parallel experiments. The conductivities of pristine spiro film without dopant was 2.94×10^{-6} S·cm^{-1} which is similar to the reported values[21]. It showed a significant increase when TBP and TFSI-Li were added, nearly two orders of magnitude times higher than pristine spiro film. The conductivity of spiro-OMeTAD is further enhanced by doping with cobalt addictives. The highest conductivity was spiro film with t-Bu Co dopant, increase from 2.11×10^{-4} to 8.38×10^{-4} S·cm^{-1}, nearly 4-fold increased compared to film without Cobalt dopant. Accordingly t-Bu Co dopant have obvious effect and perform better than dopant with MeO and Me substituted groups and got the best performance .

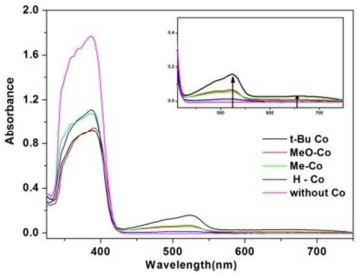

Fig.3 UV absorption spectra of spiro-OMeTAD with additives (LiTFSI and TBP) and Various Co dopant. The inset shows the enlarged spectra of the oxidized spiro-OMeTAD peak at around 523 nm. All solutions contained the same concentration of Spiro-OMeTAD (2×10^{-5} M).

To investigate the oxidation of spiro-OMeTAD by Co dopants, UV optical absorption spectroscopy was used. According to previously reported, the oxidation state of spiro would result in absorption peak around 523 nm which belonged to oxidized spiro and will not interfered by neutral spiro, spiro radical cation, and Co complexes. The UV-vis absorption spectra for spiro solution in co-solvent upon adding dopantD1, D2 , D3, D4 and without dopant（the spiro solution in co-solvent of dichloroethane and acetylacetone have added TBP and TFSI-Li） are illustrated in fig(3) . There is no absorption band of spiro-OMeTAD without dopant at 520 nm, when various Co dopants were added a new absorption band with the peak maxima located at around 523 nm was clearly observed. Additionally, we found that it has a simultaneous increase of absorption extended to 750nm which are assigned to the absorption of Spiro-OMeTAD cation, this phenomenon may attribute to the effect of both cobalt dopant and solvent. The trend of each dopant was shown in the inset of fig (3). Due to driving force for charge transport reaction of spiro-OMeTAD to the oxidation state, t-Bu Co has the strongest absorption peak, which contributes to high efficiency of spiro-to-spiro$^+$ conversion. The second absorption peak belongs to MeO-Co, followed dopants were Me-Co and H-Co. It proved that the higher absorption peak at 523 nm the dopant possesses, the more spiro$^+$ amount will generate and the result coincided with devices performance.

The solvent also had a significant impact on cells. In order to investigate the solvent effect, we screened some solvents to find an appropriative solvent for the bipyridine type co-complexes. Herein, the solvent should dissolve the spin-coating formulation of HTM, which comprises dopant, spiro-MeOTAD, lithium bis (trifluoromethylsulfonyl) imide (LiTFSI), and 4-tert-butylpyridine (TBP). It was found that the formulation was hard to be dissolved well just in only one solvent and make sure the perovskite was not corroded by solvent at the same time. Therefore we adopted a co-solvent that both of HTM and each component have good solubility. The co-solvent that consist of dichloroethane and acetylacetone (V: V=7:3) solvent (fig.1) had better solubility with co complexes that is quite different from chlorobenzene which was commonly used.

We compared D1 complexes dissolved in chlorobenzene and co-solvent respectively, as we can see from fig4(a), D1 had relatively poor solubility in chlorobenzene and the solution was cloudy due to insoluble precipitates (① in the picture), but can be dissolved well in co-solvent (③ in the picture). ②and ④ were the HTM solution with TBP, Li-TFSI and co-dopant in chlorobenzene and co-solvent respectively, and the corresponding color were dark purple and orange red. The color of pure spiro solution changed when dopants were added, and D1 dopant was different from ordinary used pyrazoles type additives which expressed dark purple. It will avoid the competition with the photosensitizer for light absorption and thus increase device performance.

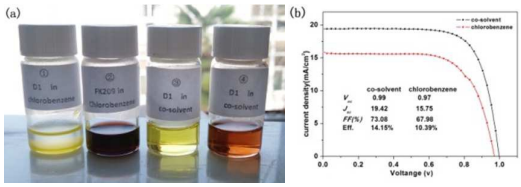

Fig.4 (a) Co-complexes (D1) with t-Bu group in different solvent. ①and ③ in the picture were co-dopant in chlorobenzene and co-solvent respectively, ② and ④ were spiro with TBP, Li-TFSI and co-dopant in chlorobenzene and co-solvent. (b) The J-V curves of D1 dopant in different solvent.

After D1 dissolved in co-solvent, the conductivity of HTM increased from 7.86×10^{-5} to 8.38×10^{-4} S·cm^{-1}, nearly 10.4-fold increased. Here we used transient absorption spectra (TAs) in order to detect the recombination time between HTM layer and TiO_2 layer. The result showed in fig5(a) and (b) , the recombination time between TiO_2 layer and spiro layer of device by using co-solvent was 34.06 μs that is longer than using chlorobenzene which only got 7.36 μs , the longer recombination time indicated lower electron-hole recombination rate. The J-V curve was shown in fig4 (b), it clearly confirmed that devices with dopant using co-solvent expressed better performance compare with using chlorobenzene.

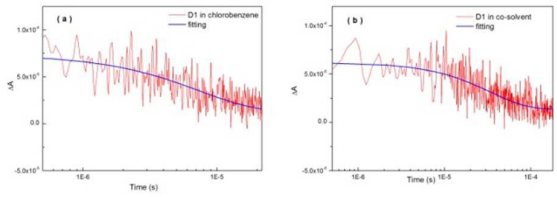

Fig.5 (a) TAs response of TiO2/ perovskite /HTM. HTM layer with D1 dopant in chlorobenzene ,which were measured with a pump light wavelength of 500 nm and a probe light wavelength of 1100 nm through detecting spiro cation. The blue solid line represents the fitting result with a one exponential function with a recombination time of 7.36μs. (b) HTM layer with D1 dopant in co-solvent, the red curves are the results of the samples without and with D1 dopant, with a recombination time of 34.06μs.

In order to determine the influence of the dopants on the photovoltaic performance, we prepared PSCs employing co-solvent in combination with Spiro-MeOTAD as hole conductor. Photovoltaic parameters of PSC are shown in fig (6).

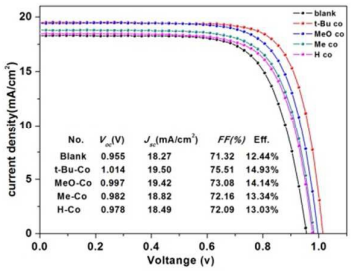

Fig. 6 Photocurrent-voltage (J-V) characteristics (light intensity: 100 mW/cm^2, AM1.5G) of various dopants. The concentration of 6% dopant was added in mol% relative to spiro-MeOTAD. The preparation of HTM formulation by mixing the solution of 75mg spiro-MeOTAD, 18μL LiTFSI, 29μL TBP in 0.7ml dichloroethane and different concentration Co-dopants(300mg/ml in MeCN) in 0.3ml acetylacetone (dichloroethane:acetylacetone= 7:3, V/V).

The corresponding photovoltaic parameters are collected in the insert table of fig (6), the PCE trend of the devices based on dopants had a slight increase. The device without Co-dopant showed a comparably low efficiency of 12.44% with a short-circuit photocurrent density (J_{SC}) of 18.27 mA/cm^2, an open-circuit photo voltage (V_{OC}) of 0.95 V, and a fill factor (*FF*) of 71.32%. The device employing D1 dopant (t-Bu-Co) as the dopant yielded an efficiency of 14.93%, which is considerably higher than the efficiencies of devices obtained based on other co-dopant dopants. It might be attributed to the increase of conductivity and charge-transport mobility in coordination with a small quantity of protons (H^+) that generated by acetylacetone during the photoinduced photochemical reactions. We note that the lowest conversion efficiency of the device using D4 dopant (H-Co) without substituted group is 13.03%, which can be mainly ascribed to its relative low *FF*, which might be a result of lower conductivity and cobalt crystallized between the interface when the film take shape.

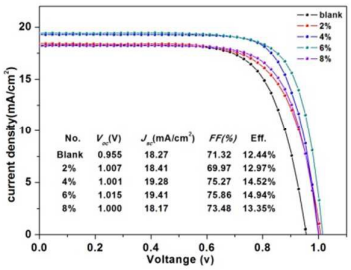

Fig.7 Photocurrent-voltage (*J-V* curve) of devices based on different concentration of doping .Percentages given in the legend was the amount of Co (III) added to the solution in mol % relative to spiro-MeOTAD.

Dopant concentrations from 0 (blank)–8mol% (the percentages are the amount of Co dopants added to the solution in mol% relative to spiro-MeOTAD) were investigated with Li-TFSI and TBP added. The corresponding *J-V* curves obtained are shown in fig (7), and the photovoltaic parameters are collected in the insert table. Devices were measured directly after device fabrication without any additional treatment. The device without dopant showed a relatively low efficiency of 12.44% after cell fabrication. Relatively low efficiency of blank sample obtained can ascribe to the low conductivity and high charge transport resistance of the nondoped hole transport layer. Through further optimization of the doping concentrations, the device fabricated with 6mol% t-Bu Co dopant showed the best performance. The J_{sc} and V_{oc} values for this device increased from18.27 mA /cm^2 to 19.41 mA /cm^2 and from 0.95V to 1.01V, yielding an overall PCE of 14.94%. This corresponds to an improvement more than 20% as compared to the efficiency of the device containing the nondoped HTM. This can be attributed to the enhanced solubility of dopant in co-solvent which will lead to a better dispersion of spiro-MeOTAD matrix, enhance charge transport and avoid the crystallization of the Co complexes salt during the spin coating process. However, J_{sc} and V_{oc} values decreased at higher concentrations (8 mol %), especially *FF*, it might be attributed to the increased recombination due to recrystalized and unreacted dopant in HTM Component.

Fig8(a) and (b) shows the J – V curves measured via reverse and forward bias sweep for one of the best-performing solar cells and the incident photon-to-current conversion efficiency (IPCE) spectra using 6 mol% dopant, the average values of device showed J_{sc} of 19.52 mA/cm^2, V_{oc} of 1.019V, and *FF* of 74.96% under AM 1.5G solar irradiance (100 mW/cm2), yielding a PCE of 14.91%, which close to the devices base on FK209 dopant (ESI.fig2). The calculated photocurrent from the IPCE spectrum is 19.37 mA /cm^2 that was agreed well with the measured J_{sc}. This study reveals that the Co-complexes can be used as an alternative way to increase the photon-to-electron conversion.

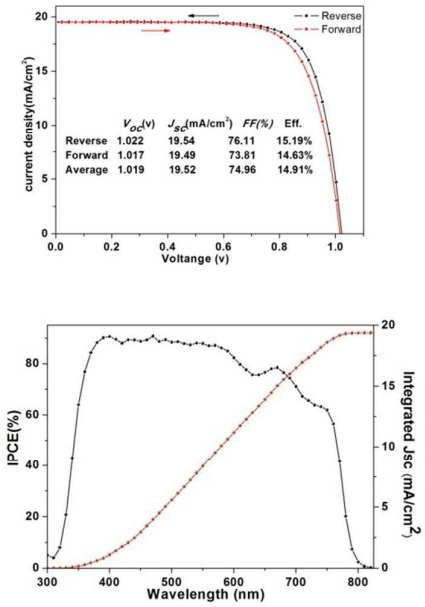

Fig. 8 *J-V* and IPCE characteristics for the best cell obtained in this study. (a) *J-V* curves of forward and reverse bias sweep for the solar cell (b) corresponding incident photon-to-current conversion efficiency (IPCE) and integrated J_{sc} spectra.

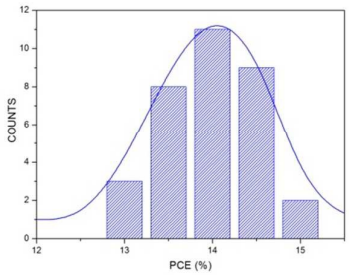

Fig.9 Histogram of devices PCE based on spiro HTM system by doping cobalt complexes in co-solvent (measured from 33 devices).

To check the reproducibility of the devices performance by using cobalt dopant, we repeated the device fabrication using the optimal doping concentration of 6% mol, photovoltaic parameters are compared using histograms obtained from 33 integrated perovskite devices shown in fig(9). As can be seen from the results, the devices performed well, the average PCE was 14.23%,and more than 80% of the devices showed PCE above 13.5% under 1 sun conditions, the average J_{SC} and V_{OC} values were highly reproducible. The PCE data obtained from the cells shows a low standard deviation, indicating good reproducibility.

Conclusions

We synthesized series substituted bipyridine cobalt complexes as HTM dopant and fabricated mesoscopic TiO_2/ $CH_3NH_3PbI_3$

heterojunction solar cells using cobalt dopant in co-solvent of dichloroethane and acetylacetone, the synthesized dopant shows excellent dopant properties in photovoltaic applications. Finally, we achieved power conversion efficiency of 14.91% using dopant under optimal conditions. The addition of co-complex to spiro-OMeTAD increased device performance mainly due to the increase of electron transport capability and solubility of HTM by using co-solvent. Furthermore, the results of this study show that the method of doping not only improves the overall device performance, but also exhibit good reproducibility. It provides new way for the fabrication low-cost and efficient perovskite solar cell. Further work on the study and the employment of this additive in different organic HTMs is on progress.

Acknowledgements

This work was financially supported by the National High Tech nology Research and Development Program of China under Grant no.2015AA050602, the National Natural Science Foundation of China under Grant no. 21273242, and State Key Laboratory of Alternate Electrical Power System with Renewable Energy Sources (Grant No.LAPS14012).

Notes and references

1. J. Burschka, N. Pellet, S.-J. Moon, R. Humphry-Baker, P. Gao, M. K. Nazeeruddin and M. Grätzel, *Nature*, 2013, **499**, 316-319.
2. B. Conings, L. Baeten, T. Jacobs, R. Dera, J. D'Haen, J. Manca and H.-G. Boyen, *APL Materials*, 2014, **2**, 081505.
3. N. J. Jeon, J. H. Noh, Y. C. Kim, W. S. Yang, S. Ryu and S. I. Seok, *Nature materials*, 2014.
4. H. Zhou, Q. Chen, G. Li, S. Luo, T.-b. Song, H.-S. Duan, Z. Hong, J. You, Y. Liu and Y. Yang, *Science*, 2014, **345**, 542-546.
5. D. Liu, J. Yang and T. L. Kelly, *Journal of the American Chemical Society*, 2014, **136**, 17116-17122.
6. H.-S. Kim, C.-R. Lee, J.-H. Im, K.-B. Lee, T. Moehl, A. Marchioro, S.-J. Moon, R. Humphry-Baker, J.-H. Yum and J. E. Moser, *Scientific reports*, 2012, **2**.
7. J.-H. Im, I.-H. Jang, N. Pellet, M. Grätzel and N.-G. Park, *Nature nanotechnology*, 2014, **9**, 927-932.
8. N. J. Jeon, H. G. Lee, Y. C. Kim, J. Seo, J. H. Noh, J. Lee and S. I. Seok, *Journal of the American Chemical Society*, 2014, **136**, 7837-7840.
9. A. Kojima, K. Teshima, Y. Shirai and T. Miyasaka, *Journal of the American Chemical Society*, 2009, **131**, 6050-6051.
10. Y. Song, S. Lv, X. Liu, X. Li, S. Wang, H. Wei, D. Li, Y. Xiao and Q. Meng, *Chemical Communications*, 2014, **50**, 15239-15242.
11. Z. Yu and L. Sun, *Advanced Energy Materials*, 2015.
12. U. Bach, D. Lupo, P. Comte, J. Moser, F. Weissörtel, J. Salbeck, H. Spreitzer and M. Grätzel, *Nature*, 1998, **395**, 583-585.
13. Y.-J. Kim, D.-T. Tung, H.-J. Choi, B.-J. Park, J.-H. Eom, K.-S. Kim, J.-R. Jeong and S.-G. Yoon, *RSC Advances*, 2015, **5**, 52571-52577.
14. Z. Liang, S. Zhang, X. Xu, N. Wang, J. Wang, X. Wang, Z. Bi, G. Xu, N. Yuan and J. Ding, *RSC Advances*, 2015, **5**, 60562-60569.
15. A. Abate, T. Leijtens, S. Pathak, J. Teuscher, R. Avolio, M. E. Errico, J. Kirkpatrik, J. M. Ball, P. Docampo and I. McPherson, *Physical Chemistry Chemical Physics*, 2013, **15**, 2572-2579.
16. J. H. Heo and S. H. Im, *physica status solidi (RRL)-Rapid Research Letters*, 2014, **8**, 816-821.
17. D. Poplavskyy and J. Nelson, *Journal of applied physics*, 2003, **93**, 341-346.
18. H. J. Snaith and M. Gratzel, *Applied physics letters*, 2006, **89**, 262114-262114-262113.
19. J. Burschka, F. Kessler, M. K. Nazeeruddin and M. Grätzel, *Chemistry of Materials*, 2013, **25**, 2986-2990.
20. J. H. Noh, N. J. Jeon, Y. C. Choi, M. K. Nazeeruddin, M. Grätzel and S. I. Seok, *Journal of Materials Chemistry A*, 2013, **1**, 11842-11847.
21. T. M. Koh, S. Dharani, H. Li, R. R. Prabhakar, N. Mathews, A. C. Grimsdale and S. G. Mhaisalkar, *ChemSusChem*, 2014, **7**, 1909-1914.
22. B. Xu, E. Gabrielsson, M. Safdari, M. Cheng, Y. Hua, H. Tian, J. M. Gardner, L. Kloo and L. Sun, *Advanced Energy Materials*, 2015.
23. J. Y. Kim, S. H. Kim, H. H. Lee, K. Lee, W. Ma, X. Gong and A. J. Heeger, *Advanced materials*, 2006, **18**, 572-576.

Table of contents

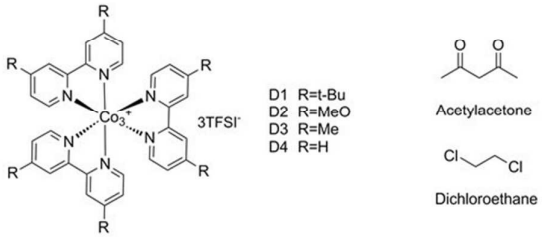

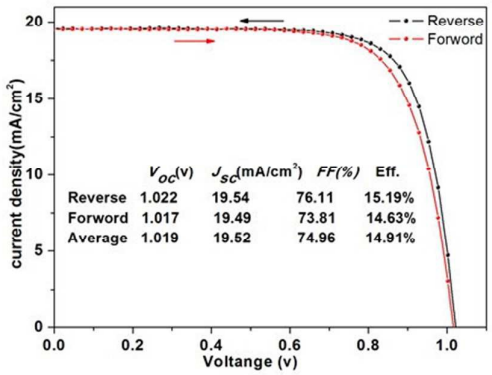

This work focus on preparing series substituted bipyridine cobalt complexes as HTM dopant and using co-solvent of dichloroethane and acetylacetone as HTM solvent. Finally, we achieved power conversion efficiency of 14.91% using dopant under optimal conditions.